

Supporting Information:

Bimetallic Docked Covalent Organic Frameworks with High Catalytic Performance towards Coupling/Oxidation Cascade Reactions

Yaling Li,^{†a} Kaiming Zuo,^{†a} Tingjun Gao,^a Jifeng Wu,^a Xiaofang Su,^a Chaoyuan Zeng,^{*a} Huanjun Xu,^{ab} Hui Hu,^a

Xiaosong Zhang^c and Yanan Gao^{*a}

1. Materials

All materials and solvents were obtained from commercial resources and used without further purification. Two building units, 5,10,15,20-tetrakis(4-aminoophenyl)porphyrin (TAPP) and 2,5-dihydroxyterephthalaldehyde (Dha) were synthesized according to published procedures.^{S1,S2}

2. Synthesis of TAPP-PA-COF

TAPP (27 mg, 0.04 mmol) and 1,4-phthalaldehyde (PA) (10.8 mg, 0.08 mmol) were placed in a glass ampule vessel (10 mL), followed by adding a solution of 1,2-dichlorobenzene (o-DCB)/n-butanol (1/1 by vol.; 2 mL). The mixture was sonicated for 5 min and the vessel was then flash frozen in liquid nitrogen. After that, 0.2 mL of 6.0 M acetic acid was rapidly added into the vessel. The reaction system was flash frozen in liquid nitrogen bath to degas by freeze-pump-thaw for three cycles. The internal pressure of the vessel was controlled below 5 Pa. The vessel was rapidly sealed with a flame, and then heated at 120 °C for 3 days. After the reaction, the COF powder was filtered out, washed with tetrahydrofuran, N,N-dimethylformamide and acetone and dried under vacuum at 120 °C for 10 h to give purple powder in 87% yield. The crystallization of the TAPP-COF was characterized by PXRD, as shown in Fig S1.

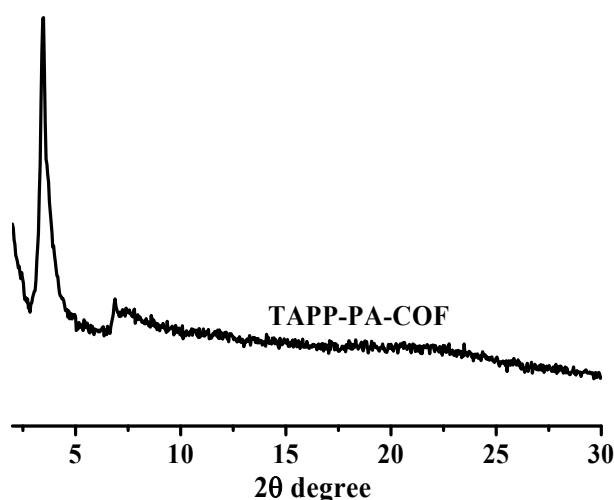


Fig S1. PXRD of TAPP-PA-COF.

3. Synthesis of Cu(II)@TAPP-PA-COF

50 mg of freshly prepared TAPP-PA-COF was treated with 20 mg of copper acetate monohydrate dissolved in dried methanol (30 mL). The mixture was stirred at 50 °C for 24 h. The precipitate was collected by filtration and washed several times with methanol, dichloromethane, then dried under vacuum to give 51.3 mg dark-purple Cu(II)@TADP-COF powder. The yield

was calculated to be 96%. The theoretical Cu content in the COF was calculated based on a porphyrin unit in the COF, which is 6.9 wt%.

4. Synthesis of Pd(II)@TAPP-PA-COF

50 mg of freshly prepared TAPP-PA-COF was treated with 30 mg of palladium acetate monohydrate dissolved in dried methanol (30 mL). The mixture was stirred at 50 °C for 24 h. The precipitate was collected by filtration and washed several times with methanol, dichloromethane, then dried under vacuum to give 76.0 mg dark Pd(II)@TADP-COF powder. The Pd(II)@TAPP-PA-COF yield was calculated to be 93%. The theoretical Pd content in the COF was calculated based on a porphyrin unit and four imine groups in the COF, which is 22.3 wt%.

5. The metal contents in COFs.

In a similar way, the Cu content in the Cu(II)@TADP-COF was calculated to be $64 \times 2 / [1029] = 12.4$ wt%; the Cu content in Pd(II)/Cu(II)@TADP-COF was calculated to be $64 \times 2 / [1253] = 10.2$ wt%; and the Pd content in Pd(II)/Cu(II)@TADP-COF was calculated to be $106 / [1253] = 8.4$ wt%.

6. The crystalline structure of TADP-COF.

The COF models were generated using the vertex positions from the Reticular Chemistry Structure Resource. The unit cell structures (e.g., cell parameters, atomic positions, and total energies) of TADP-COF were calculated using the density-functional tight-binding (DFTB) method, as implemented in the DFTB+ program package. Pawley refinement was carried out using Reflex, a software package for crystal determination from XRD pattern. Unit cell dimension was set to the theoretical parameters. The Pawley refinement was performed to optimize the lattice parameters iteratively until the wRp value converges. The pseudo-Voigt profile function was used for whole profile fitting and Berrar–Baldinozzi function was used for asymmetry correction during the refinement processes. Line broadening from crystallite size and lattice strain was both considered.

As for the possible crystal structure of TADP-COF, we have taken into accounts two possible models: model 1, Dha on top of Dha and PA on top of PA between the layers, and model 2: Dha on top of PA and PA on top of Dha between the layers. We compared the energy of the two models through theoretical calculations using DFTB method and found that the energy of the model 1 is -91.2 kcal/mol lower than that of model 2 (see Fig 2 and 3). So, we believe that the model 1 is more reasonable.

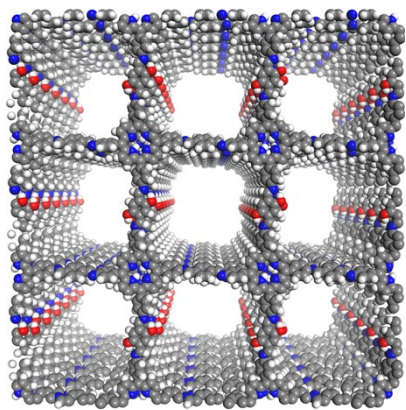


Fig S2: model 1, Dha on top of Dha and PA on top of PA between the layers

$E_{\text{total}} = -179745.2$ kcal/mol

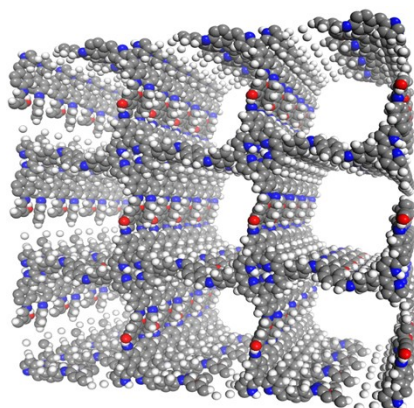


Fig S3: model 2, Dha on top of PA and PA on top of Dha between the layers

$E_{\text{total}} = -179653.5$ kcal/mol

Thus, $dE = (-179745.2) - (-179653.5) = -91.2$ kcal/mol.

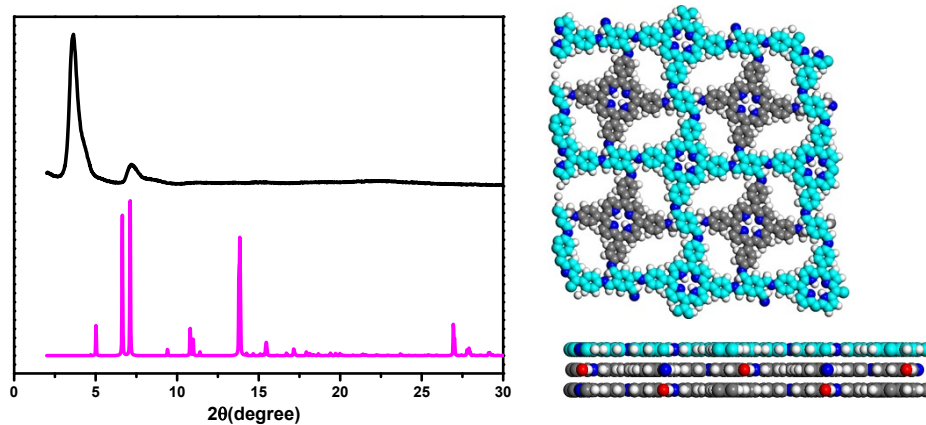


Fig S4. Observed PXRD pattern (black), and simulated PXRD pattern (magenta) for an AB stacking structure.

Table S1 Fractional atomic coordinates for the unit cell of TADP-COF.

| Monoclinic P2/M | | | |
|---|----------|---------|---------|
| a = c = 24.52 Å, b = 3.79 Å | | | |
| $\alpha = \gamma = 90^\circ, \beta = 88.92^\circ$ | | | |
| H1 | 0.04498 | 0.00000 | 0.00980 |
| C2 | 0.07987 | 0.00000 | 0.41332 |
| C3 | 0.16597 | 0.00000 | 0.06219 |
| C4 | 0.42882 | 0.00000 | 0.90539 |
| C5 | 0.06806 | 0.00000 | 0.83588 |
| C6 | 0.86818 | 0.00000 | 0.98461 |
| C7 | 0.92212 | 0.00000 | 0.90816 |
| C8 | 0.86617 | 0.00000 | 0.89278 |
| N9 | 0.92125 | 0.00000 | 0.96464 |
| C10 | -0.03623 | 0.00000 | 0.86696 |
| C11 | -0.05820 | 0.00000 | 0.80912 |
| C12 | -0.01526 | 0.00000 | 0.77212 |
| C13 | -0.01745 | 0.00000 | 0.71687 |
| C14 | -0.06786 | 0.00000 | 0.69002 |
| C15 | 0.88568 | 0.00000 | 0.72376 |
| C16 | 0.89048 | 0.00000 | 0.78045 |
| N17 | -0.06090 | 0.00000 | 0.63500 |
| C18 | 0.96148 | 0.00000 | 0.54379 |
| C19 | 0.01923 | 0.00000 | 0.55354 |
| C20 | 0.05615 | 0.00000 | 0.51028 |
| O21 | 0.04367 | 0.00000 | 0.60308 |
| H22 | 0.01557 | 0.00000 | 0.63170 |
| H23 | 0.02159 | 0.00000 | 0.69545 |
| H24 | 0.02360 | 0.00000 | 0.78934 |
| H25 | 0.84458 | 0.00000 | 0.70597 |
| H26 | 0.84984 | 0.00000 | 0.79815 |
| H27 | 0.87557 | 0.00000 | 0.57479 |
| H28 | 0.09995 | 0.00000 | 0.51935 |
| H29 | 0.07675 | 0.00000 | 0.79228 |
| H30 | 0.15163 | 0.00000 | 0.83839 |
| C31 | 0.97695 | 0.00000 | 0.12288 |
| C32 | 0.89550 | 0.00000 | 0.07974 |
| C33 | 0.88464 | 0.00000 | 0.13721 |
| N34 | 0.95204 | 0.00000 | 0.07263 |
| C35 | 0.85193 | 0.00000 | 1.04084 |
| C36 | 0.79194 | 0.00000 | 0.05662 |

| | | | |
|-----|---------|---------|---------|
| C37 | 0.74779 | 0.00000 | 1.01873 |
| C38 | 0.69245 | 0.00000 | 1.03129 |
| C39 | 0.67389 | 0.00000 | 1.08564 |
| C40 | 0.71618 | 0.00000 | 0.12452 |
| C41 | 0.77092 | 0.00000 | 0.11087 |
| N42 | 0.62188 | 0.00000 | 1.10766 |
| C43 | 0.53807 | 0.00000 | 0.04426 |
| C44 | 0.55608 | 0.00000 | 0.98978 |
| C45 | 0.51886 | 0.00000 | 0.94714 |
| H46 | 0.59952 | 0.00000 | 0.97991 |
| H47 | 0.66438 | 0.00000 | 0.99662 |
| H48 | 0.75356 | 0.00000 | 0.97523 |
| H49 | 0.70544 | 0.00000 | 0.16803 |
| H50 | 0.79541 | 0.00000 | 0.14721 |
| H51 | 0.54231 | 0.00000 | 0.13080 |
| H52 | 0.53429 | 0.00000 | 0.90497 |
| H53 | 0.79052 | 0.00000 | 0.93211 |
| H54 | 0.84690 | 0.00000 | 0.85385 |

References

- S1. Q. Sun, B. Aguila and S. Ma, *Mater. Chem. Front.*, 2017, **1**, 1310–1316.
- S2. C. Xu, J. Lin, D. Yan, Z. Guo, D. J. Austin Jr, H. Zhan, A. Kent and Y. Yue, *ACS. Appl. Nano Mater.*, 2020, **3**, 6416–6422.